Peertechz

CLINICAL GROUP

INTERNATIONAL JOURNAL OF
Radiology and Radiation Oncology
OPEN ACCESS JOURNAL

ISSN: 2640-7566 DOI: https://dx.doi.org/10.17352/ijrro

Research Article

A retrospective study of SPECT/CT scans using SUV measurement of the normal lumbar vertebrae with Tc-99m methylene diphosphonate

Ruifeng Wang[1], Cong Shen[2], Dong Han[1], Zhaoguo Zhang[1], Yuhong Zeng[3], Hulin Wu[1], Xiaotong Xu[1], Tao Qin[1], Nan Yu[1], Yongjun Jia[1], Pengtian Zhang[1], Taiping He[1], Guo youmin[2] and Yan Feng[3]*

[1]Department of Medical Image, the Affiliated Hospital of Shanxi University of Chinese Medicine, Shananxi, China

[2]Department of Medical Image, the First Affiliated Hospital of Xi'an Jiaotong University, Xi'an, China

[3]Department of Osteoporosis, Honghui Hospital, Xi'an Jiaotong University, Xi'an, China

Received: 08 March, 2021
Accepted: 05 April, 2021
Published: 07 April, 2021

***Corresponding author:** Yan Feng, Department of osteoporosis, Honghui Hospital, Xi'an Jiaotong University, No. 555 East Youyi Road, Xi'an City, Shaanxi, 710054, China, Tel: +86 29 62818587;
E-mail: 465040532@qq.com

Keywords: Bone; Lumbar vertebra; SPECT/CT; Standardized uptake value; Methylene diphosphonate

https://www.peertechzpublications.com

Abstract

Objective: The aim of this study was to acquire the SUVs for each segment of the vertebral body to explore the rationale for the large variability of the SUVs in normal vertebrae.

Methods: This retrospective study was performed using the images and data from 39 cancer patients who underwent bone SPECT/CT scans with Tc-99m MDP. The SUVmax and SUVmean of the anterior, middle, posterior; left, middle, right; top, middle, and lower of the lumbar vertebrae 1~5, were calculated. The continuous variables were represented by the median values (Q1,Q3), and the differences among various segments were analyzed by Friedman's nonparametric test. The pairwise comparison between groups was corrected by the Bonferroni method. The $P<0.05$ was considered statistically significant.

Results: In this study, 39 patients (31 women and 8 men; mean age, 54.79±9.12 years; age range, 39–71 years) were elucidated. The SUVmax of the L1 and L3 vertebral bodies' parts were significantly different from those of the other portions of the same lumbar vertebra. The SUVmax of the lower posterior portion of the L1 vertebral body was significantly different from that of the upper posterior portion. There were significant differences in the SUVmax between the upper and lower portions, middle and lower portions in the middle of the L3 vertebral body. The SUVmean of the lower posterior portion of L1 and L2 vertebral were significantly different from those of the upper posterior portion. There were significant differences in the SUVmean between the upper and lower portions of the middle of the L3 vertebral body. There were significant differences among the SUVmax and SUVmean of the right, and middle of the vertebral body except for the L2 vertebral body. There were significant differences among the SUVmax and SUVmean of the anterior, middle segments of the lumbar vertebrae body, and the SUVmax of the anterior and posterior parts of the L2 vertebral body, and the SUVmean of the middle and posterior parts of the L1 vertebra. The SUVmax of the middle and posterior portions of the L3～L5 vertebral body, and the SUVmean of the L1～L3, and L5 lumbar vertebrae had significant differences.

Conclusion: The difference in the bone metabolism of the lumbar vertebral body is caused by the variation in the horizontal direction of the vertebral body. The bone metabolism in the vertical direction of the lumbar vertebrae has more uniformity. As a quantitative imaging measure, the SUVs might require standardization with adequate reference data to minimize the variability in the participants.

Citation: Wang R, Shen C, Han D, Zhang Z, Feng Y, et al. (2021) A retrospective study of SPECT/CT scans using SUV measurement of the normal lumbar vertebrae with Tc-99m methylene diphosphonate. Int J Radiol Radiat Oncol 7(1): 022-029. DOI: https://dx.doi.org/10.17352/ijrro.000046

Abbreviations

MDP: Methylene Diphosphonate; SPECT/CT: The Single-Photon Emission Tomography /Computed Tomography; QIB: Quantitative Imaging Biomarker; SUV: Standardized Uptake Value; DJD: Degenerative Joint Disease; VOI: Volume Of Interest; WBS: Whole-Body Scan; BCF: Becquerel Calibration Factor

Introduction

The skeleton is the most frequent site for tumor metastasis. The extent of metastasis is the prognostic indicator in cancer patients following treatment [1,2]. Various types of tumors cause the different relative incidence of bone metastasis and the median-survival time in cancer patients [3]. The spine and pelvis are the most common sites for secondary bone metastases for different primary cancers [2,4].

The Technetium-99m labeled bone scintigraphic agent Methylene Diphosphonate (MDP) which binds to the mineral phase of bone hydroxyapatite and the calcium-rich tissue has been widely used in bone scintigraphy in metastatic bone diseases in the past [5,6]. Planar imaging has been mainly performed in bone scintigraphy, and Single-Photon Emission Computed Tomography (SPECT) has also been performed in body parts with a limited range of clinical diagnosis value. The Single-Photon Emission Tomography (SPECT)/Computed Tomography (CT) scanner combining SPECT and Computed Tomography (CT) has gained widespread acceptance. The SPECT/CT scanner provides fusion images of CT and SPECT and produces attenuation correction maps necessary for quantitative analysis using the Standardized Uptake Value (SUV) [2,5,7,8]. The SUV integrates the concept of biomarker and the notion of quantitative imaging. A Quantitative Imaging Biomarker (QIB) uses objectively measured characteristics derived from an *in vivo* image and serves as an indicator of normal biological processes, pathological processes, or response to a therapeutic intervention [8]. The Quantitative measurements which have been defined as the extraction of quantifiable features from the medical images to determine the normality or the degree of alteration, or the status of a disease, injury, or chronic condition relative to the normal have been vastly used with the advances in molecular imaging [8,9].

The bone scans of vertebrae were quantitatively analyzed using the SUV as QIB of SPECT/CT scans with Tc-99m-MDP [5,8,10,11]. Jun Zhao's study evaluated SUVmax and SUVmean of benign bone lesion and malignant bone metastasis foci of normal vertebrae, which provide a quantitative reference for clinical diagnosis and the evaluation of therapeutic response in vertebral lesions [12]. The bone tissue blood flow and osteoblastic activity is proportional to bone tissue uptake of 99mTc-MDP [13,14]. bones at different sites can have different normal SUVs [5,8]. SUVmax and SUVmean were proved to be significantly different between male and female patients in most vertebrae [12]. Hence, as a quantitative imaging biomarker, SUVs of normal vertebrae showed relatively large variabilities [5,14]. The SUVs for each vertebral level are different with significant variabilities [2]. Thus, it is critical to elucidate how to reduce the large variability of the SUV of normal vertebrae. The huge variability of SUVs in a lumbar vertebra may have resulted from the uneven metabolism in the vertebral body. Therefore, the primary aim of this study was to elucidate the SUVs for each segment of the vertebral body to explore the rationale behind the large variability of SUVs in normal vertebrae.

Materials and methods

Patients

In this study, we retrospectively analyzed the imaging data of patients who underwent bone scans to explore the metastasis from various cancers such as prostate cancer, pancreatic cancer, breast cancer, colon cancer, renal cancer, lung cancer, gastric cancer, and ovarian cancer in the department of Medical Image affiliated to the Hospital of the Shanxi University of Chinese Medicine. Prior to the onset of this study, the Ethics Committee of the institution approved the study protocol. Further, informed consent from patients was obtained to use the imaging data for the research purpose. Briefly, planar and SPECT/CT images were acquired about 3-4h after intravenous injection of Tc-99m-MDP. The area of the abdomen for the SPECT/CT acquisition was determined based on the patient's disease or the purpose of the examination. The data of patients with a normal lumbar vertebra who underwent bone scans were retrospectively retrieved and analyzed. Data were acquired from a group of patients undergoing Tc-99m-MDP (Guangdong Xiai nuclear pharmaceutical Co. Ltd., Xi'an, Shaanxi, China) bone SPECT/CT between August 2016 and October 2020. The patients in group were included based on the criteria according to the referred to the literature [5]: (1) access to data on measured injection activity, time of measurement, and time of injection; (2) access to patient's weight and height information; (3) SPECT/CT that was scanned for the lumbar vertebra. The following set of exclusion criteria was outlined to determine the normal vertebrae: compression fractures, diffuse bone metastasis, ankylosing spondylitis, and metabolic bone disease. Besides, the Degenerative Joint Disease (DJD) of the spine was also characterized by correlating the tracer uptake with its CT morphological image, which encompassed osteophytes, end plates, facet joints, and the area around the joints.

Data acquisition and reconstruction

The Symbia T16 system (CT with a maximum of 16-slice acquisitions per rotation, Siemens Healthineers Molecular Imaging, Hoffman Estates, IL, USA) system was used to obtain SPECT/CT scans. The SPECT scans were acquired using low-energy high-resolution collimation, a 128×128 matrix of 4.8-mm pixel size, and a total of 450s/rotation in a continuous-rotation mode. After the SPECT acquisition, a low-dose CT scan was acquired with 130 kV and 15 ref mAs using adaptive dose modulation (CARE Dose 4D; Siemens Healthineers Molecular Imaging). The CT data were generated with 1.5 mm slice thickness using a smooth reconstruction B70s kernel. The SPECT reconstruction was performed using filtered back projection, and the attenuation correction was based on the attenuation maps derived from the CT data filtered by the B70s kernel.

Citation: Wang R, Shen C, Han D, Zhang Z, Feng Y, et al. (2021) A retrospective study of SPECT/CT scans using SUV measurement of the normal lumbar vertebrae with Tc-99m methylene diphosphonate. Int J Radiol Radiat Oncol 7(1): 022-029. DOI: https://dx.doi.org/10.17352/ijrro.000046

The delineation of the Volume of Interest (VOI) was performed by a board-certified radiologist using a software "Dynamic Analysis" purchased from Beijing Dynamic Analysis Medical Information Technology Co. Ltd. (Beijing, China) which reports the statistics for the various SUVmax, SUVmean. The VOIs that covered the vertebral body were hand-drawn. All data were decay-corrected to the time of injection to control fluctuations of the start time of the acquisition. Final values of quantitative tracer concentrations were thus defined concerning the injection time. The patient's clinical data were acquired from the Hospital Information System (HIS) database.

SPECT/CT image analysis

The Whole-Body Scan (WBS) and SPECT/CT images were independently interpreted by two experienced nuclear medicine professors and a diagnostic radiologic professor. In cases of discrepancies, the consensus was obtained by a joint reading. The SUVs of 39 lumbar vertebrae were included for the analyses based on the previously defined criteria [5]. The patients were included based on the following criteria: (1) access to data on measured injection activity, time of measurement, and time of injection; (2) access to patient's weight and height information; (3) SPECT/CT scans had the lumbar vertebrae; and (4) absence of diffuse bone metastases, ankylosing spondylitis, metabolic bone disease, and osteoarthritis.

A square box with a side length of 2.71 cm (20 mL) filled with a Tc-99m MDP solution of known active concentration (approximately 2 mCi) was scanned. The data were reconstructed with the filtered back-projection and the CT-based attenuation correction and then processed with SPECT/CT cameras. The SPECT/CT data were analyzed using a software "Dynamic Analysis" (Beijing Dynamic Analysis Medical Information Technology Co. Ltd., Beijing, China). The slice thickness automatically converted to be about 1.5 mm to allow isotropic voxel evaluation. A rectangular region of interest (ROI) was drawn on the cubic phantom in the central slice, measuring the SPECT count density (count/cc). The calibration factor was calculated as the ratio of actual radioactivity concentration (as measured by the dose calibrator) in the square box at the time of scanning to the measured SPECT count density per scan duration; this factor is known as the Becquerel calibration factor (BCF). The BCF is calculated as follows:

$$BCF\ [Bq / cps] = ACC\ [-Bq / cc]/MC\ [count/cc \times 1 / sec]$$

The patients were scanned using the SPECT/CT system. The patient's data in the reconstruction condition were analyzed using the same software as BCF data. The VOIs were plotted by manually adjusting the boundary of VOIs of the SPECT and the boundary of the spongy bone of the vertebral body on the CT boundaries of the fused SPECT/CT images. Then, SUVmax and SUVmean were measured [7].

The SUV was calculated as follows:

$$SUV = BCF_{[Bq/cps]} \times MC_{[count/cc \times 1/Sec]} \times \frac{Body\ weight_{[g]}}{Injected\ activity_{[Bq]}}$$

The vertebral body was manually dived into three parts: anterior, middle, posterior;left, middle and right; top, middle, and bottom and the SUV values of each part of the vertebral body were measured, respectively. The SPECT/CT system was calibrated with a uniform phantom, which provided a volume sensitivity factor and was specific to the camera type, collimator type, and window energy settings used. The patient's reconstructed values were then normalized with volume sensitivity. All data were decay corrected to the time of injection to control fluctuations of the start time of the acquisition. The final values of the quantitative tracer concentrations were thus defined concerning the injection time.

Statistical analysis

Shapiro-Wilk test was used to determine the normal distribution of the data. The continuous variables with normal distribution were expressed as mean ± standard deviation, and one-way repeated measures of variance analyzed the differences among different groups. The continuous variables that did not follow the normal distribution were represented by the median values (Q1,Q3), and Friedman's nonparametric test analyzed differences among various groups. The pairwise comparison between groups was corrected by the Bonferroni method. The $P<0.05$ was considered statistically significant. All analyses were computed using the SPSS v16.0 software (SPSS, Chicago, IL, USA). We used the Nonparametric pound-wise Multiple Comparisons module of PASS software to calculate the sample size.

Results

We used the Nonparametric Pair-Wise Multiple Comparisons module of PASS software to calculate the sample size.This study lumbar vertebral body SUVs between different location does not meet the normal distribution. Therefore, non-parametric tests were used to compare the differences.Assuming two comparison between three different positions, we are under the premise of type I error is less than 0.05, found 80% of the master degree of 0.5 units of the difference between any two locations, at least need to 32 cases of samples. The results are shown that 39 patients were collected retrospectively, which met the minimum sample requirements.

In this study, 39 patients (31 women and 8 men; mean age, 54.97±7.69 years; age range, 39–71 years) were included from staging malignancies, such as prostate cancer, pancreatic cancer, breast cancer, lung cancer, gastric cancer, and ovarian cancer (Table 1). The lumbar vertebrae were divided into three equal parts, upper, middle, and lower parts. The SUVmax and SUVmean of the various parts of the normal lumbar vertebrae including the anterior, middle, and posterior area of the lumbar vertebra were measured based on the body weight (Figures 1-4). The normality test of all parameters showed that parameters did not obey normal distribution ($P<0.001$). The continuous variables that were not subject to normal distribution were expressed as median values (Q1,Q3). The SUVmax and SUVmean of the the anterior, middle, posterior; left, middle, right; top, middle, and lower, are shown in Tables 2,3. The SUVmax of the lower posterior portion of the

Citation: Wang R, Shen C, Han D, Zhang Z, Feng Y, et al. (2021) A retrospective study of SPECT/CT scans using SUV measurement of the normal lumbar vertebrae with Tc-99m methylene diphosphonate. Int J Radiol Radiat Oncol 7(1): 022-029. DOI: https://dx.doi.org/10.17352/ijrro.000046

L1 vertebral body was significantly different from that of the upper posterior portion. In the SUVmax values between the upper and lower portions, middle and lower portions in the middle of the L3 vertebral body were significant differences. The SUVmean values of the lower posterior portion of L1 and L2 vertebral bodies were significantly different from those of the upper posterior portion. SUVmean values between the upper and lower portions of the middle of the L3 vertebral body had significant differences.

There were significant differences among SUVmax and SUVmean of the right, and middle of L1, L3, L4, and L5 vertebral bodies, but the SUVmax and SUVmean of the L2 vertebral body have no significant differences between the right and the middle portions. Significant differences were widely observed among the SUVmax of the middle and the left portions of the L1 vertebra, the SUVmean of the right and the left portions of the L1 and L4 vertebrae, and the SUVmean of the middle and left parts of the L3 vertebral body (Table 4,5). SUVmax

Table 1: Patient characteristics.

Characteristics	Number	Mean ± SD
Age (years-old)	39-71	54.97±7.693
Male	8	
Female	31	
Height (cm)	150-173	160.69±6.296
Body weight (kg)	35-88	58.756±9.6987
Pre-study radiotherapy only	0	
Pre-study chemotherapeutic drug	10	
Pre-study radiotherapy and chemotherapeutic drug	12	
Pre-study no radiotherapy or chemotherapeutic drug	17	
Histology		
Breast Cancer	23	
Rectal cancer	3	
Pancreatic cancer	2	
Ovarian cancer	4	
Prostate cancer	3	
Gastric cancer	1	
Lung cancer	2	
Non-neoplastic patient	1	

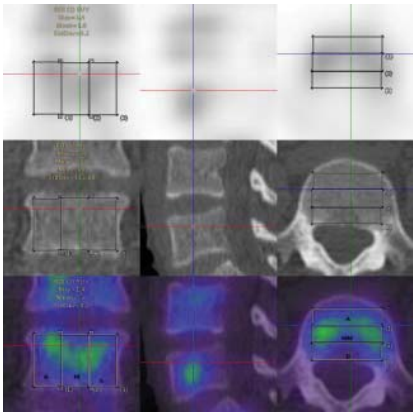

Figure 1: Transaxial, sagittal, and coronal images of a patient's SPECT/CT combined data of a lumbar vertebra. The VOIs of the lumbar vertebra were plotted by manually adjusting the boundary of the SPECT and that of the spongy bone of the lumbar vertebra on CT images. R represents right group; M represents middle group, L represents the left group, A represents anterior parts of lumbar vertebrae, MM represents middle parts of lumbar vertebrae, and P represents posterior parts of lumbar vertebrae.

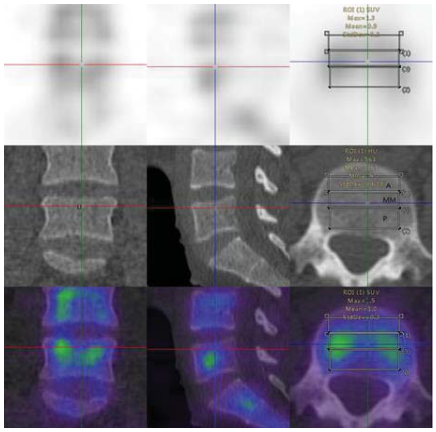

Figure 2: Transaxial, sagittal, and coronal images of a patient's SPECT/CT combined data of a lumbar vertebra. The VOIs of the upper positions of lumbar vertebra were plotted by manually adjusting the boundary of the SPECT and that of the spongy bone of the lumbar vertebra on CT images. U represents the upper group, A represents anterior parts of lumbar vertebrae, MM represents middle parts of lumbar vertebrae, and P represents posterior parts of lumbar vertebrae.

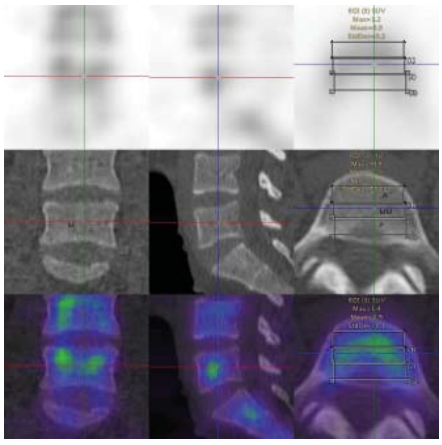

Figure 3: Transaxial, sagittal, and coronal images of a patient's SPECT/CT combined data of a lumbar vertebra. The VOIs of middle positions of the lumbar vertebra were plotted by manually adjusting the boundary of the SPECT and that of the spongy bone of the lumbar vertebra on CT images. M represents the middle group, A represents anterior parts of lumbar vertebrae, MM represents middle parts of lumbar vertebrae, and P represents posterior parts of lumbar vertebrae.

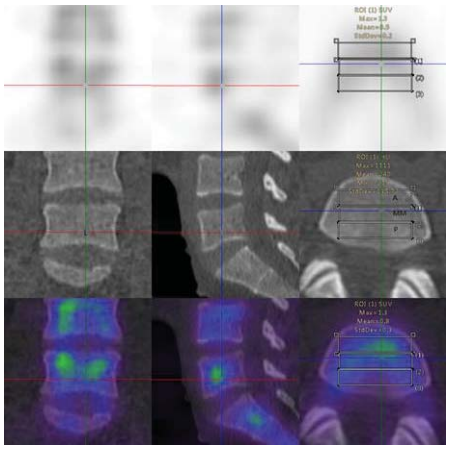

Figure 4: Transaxial, sagittal, and coronal images of a patient's SPECT/CT combined data of a lumbar vertebra. The VOIs of lower positions of the lumbar vertebra were plotted by manually adjusting the boundary of the SPECT and that of the spongy bone of the lumbar vertebra on CT images. L represents the and lower group, A represents anterior parts of lumbar vertebrae, MM represents middle parts of lumbar vertebrae, and P represents posterior parts of lumbar vertebrae.

Citation: Wang R, Shen C, Han D, Zhang Z, Feng Y, et al. (2021) A retrospective study of SPECT/CT scans using SUV measurement of the normal lumbar vertebrae with Tc-99m methylene diphosphonate. Int J Radiol Radiat Oncol 7(1): 022-029. DOI: https://dx.doi.org/10.17352/ijrro.000046

and SUVmean of the anterior, the middle parts of the L1~L5 vertebral bodies, and the SUVmax of the L2 vertebral body significant differences between the anterior and the posterior areas. SUVmean values of the middle and posterior areas of the L1 vertebra body had significant differences. The SUVmax of the middle and the posterior portions of the L3~L5 vertebral bodies, and the SUVmean of the L1~L3 vertebral bodies, and the L5 vertebral body have significant differences (Tables 6,7).

Table 2: The SUVmax value comparison of the upper, middle, and lower positions of the same vertebral.

Lumbar	Position	Upper	Middle	Lower
L1 (n=36)	A (n=36)	0.9 (0.7, 1.3)	0.9 (0.7, 1.25)	0.9 (0.8, 1.3)
	MM (n=36)	0.9 (0.73, 1.2)	0.95 (0.8, 1.3)	1 (0.8, 1.28)
	P (n=36)	0.9 (0.73, 1.08)	0.9 (0.73, 1.2)	1 (0.8, 1.28)*
L2 (n=38)	A (n=38)	1 (0.7, 1.2)	0.95 (0.8, 1.2)	0.95 (0.8, 1.23)
	MM (n=38)	1 (0.8, 1.2)	1 (0.8, 1.23)	1 (0.8, 1.3)
	P (n=38)	1 (0.8, 1.2)	0.95 (0.8, 1.2)	1 (0.88, 1.3)
L3 (n=39)	A (n=39)	1 (0.8, 1.3)	1.1 (0.8, 1.4)	1.1 (0.8, 1.3)
	MM (n=39)	1.1 (0.8, 1.3)	1 (0.8, 1.4)	1.1 (0.9, 1.4)*#
	P (n=39)	1 (0.8, 1.3)	1 (0.9, 1.3)	1 (0.8, 1.3)
L4 (n=39)	A (n=39)	1.2 (0.9,1.4)	1.1 (0.9, 1.4)	1.2 (1, 1.4)
	MM (n=39)	1.2 (1, 1.4)	1.2 (1, 1.5)	1.2 (1, 1.5)
	P (n=39)	1.1 (1, 1.4)	1.1 (1, 1.5)	1.1 (1, 1.5)
L5 (n=37)	A (n=37)	1 (0.9, 1.35)	1 (0.9, 1.4)	1.1 (0.8, 1.4)
	MM (n=37)	1.1 (0.9, 1.35)	1.1 (0.9, 1.4)	1.1 (0.9, 1.45)
	P (n=37)	1 (0.9, 1.3)	1 (0.9, 1.4)	1 (0.9, 1.3)

Note: Continuous variables were expressed as median values (Q1, Q3), and the pair comparison was corrected by the Bonferroni method. * represents a statistical difference compared with the upper group; # represents a statistical difference compared with the middle group

Table 3: The SUVmean value comparison of the upper, middle, and lower positions of the same vertebral body.

Lumbar	Position	Upper	Middle	Lower
L1 (n=36)	A (n=36)	0.7 (0.5, 0.88)	0.7 (0.5, 0.88)	0.7 (0.6, 0.88)
	MM (n=36)	0.8 (0.6, 0.98)	0.8 (0.6, 0.98)	0.8 (0.63, 1)
	P (n=36)	0.7 (0.53, 0.8)	0.7 (0.6, 0.9)	0.7 (0.6, 0.88)
L2 (n=38)	A (n=38)	0.7 (0.58, 0.9)	0.7 (0.6, 1)	0.7 (0.5, 1)
	MM (n=38)	0.8 (0.6, 1)	0.8 (0.68, 1.1)	0.8 (0.6, 1.1)
	P (n=38)	0.7 (0.6, 0.9)	0.7 (0.6, 1)	0.7 (0.6, 0.93)*
L3 (n=39)	A (n=39)	0.8 (0.6, 1)	0.8 (0.6, 1)	0.8 (0.6, 1)
	MM (n=39)	0.9 (0.7, 1.1)	0.9 (0.7, 1.1)	0.9 (0.7, 1.1)*
	P (n=39)	0.8 (0.6, 0.9)	0.7 (0.6, 1)	0.8 (0.6, 1)
L4 (n=39)	A (n=39)	0.9 (0.7, 1)	0.9 (0.6, 1)	0.9 (0.7, 1.1)
	MM (n=39)	0.9 (0.8, 1.1)	0.9 (0.7, 1.2)	0.9 (0.8, 1.2)
	P (n=39)	0.8 (0.7, 1)	0.8 (0.7, 1)	0.8 (0.7, 1.1)
L5 (n=39)	A (n=37)	0.7 (0.6, 0.95)	0.8 (0.65, 1.05)	0.8 (0.6, 1)
	MM (n=37)	0.8 (0.7, 1.05)	0.9 (0.75, 1.1)	0.8 (0.7, 1.05)
	P (n=37)	0.7 (0.7, 0.95)	0.8 (0.6, 1)	0.7 (0.6, 0.95)

Note: Continuous variables were expressed as median values (Q1, Q3), and the pair comparison was corrected by the Bonferroni method. * represents a statistical difference compared with the upper group; # represents a statistical difference compared with the middle group

Table 4: Comparison of the SUVmax values in the right, middle and left parts of lumbar vertebrae.

Lumbar	Right	Middle	Left
L1 (n=36)	1 (0.8, 1.2)	1 (0.8, 1.2)*	0.9 (0.8, 1.2)#
L2 (n=38)	1 (0.8, 1.2)	1 (0.8, 1.23)	1 (0.8, 1.3)
L3 (n=39)	1.1 (0.85, 1.4)	1.1 (0.8, 1.35)*	1.1 (0.9, 1.35)
L4 (n=39)	1.1 (1, 1.4)	1.1 (0.9, 1.3)*	1.2 (1, 1.4)
L5 (n=39)	1.1 (0.9, 1.3)	1 (0.8, 1.3)*	1.1 (0.9, 1.4)

Note: Continuous variables were expressed as median values (Q1, Q3), and the pair comparison was corrected by the Bonferroni method. * represents a statistical difference compared with the Right group, # represents a statistical difference compared between the Middle group and Left group

Table 5: Comparison of the SUVmean values in the right, middle and left portions of lumbar vertebrae.

Lumbar	Right	Middle	Left
L1 (n=36)	0.8 (0.6, 0.9)	0.8 (0.6, 0.9)*	0.7 (0.6, 0.9)*
L2 (n=38)	0.7 (0.6, 1)	0.7 (0.6, 1)	0.7 (0.6, 0.9)
L3 (n=39)	0.9 (0.6, 1.1)	0.8 (0.6, 1)*	0.8 (0.6, 1)#
L4 (n=39)	0.8 (0.7, 1.1)	0.8 (0.6, 1)*	0.9 (0.7, 1)*
L5 (n=39)	0.8 (0.6, 1)	0.8 (0.6, 1)*	0.8 (0.6, 1)

Note: Continuous variables were expressed as median (Q1, Q3), and the pair comparison was corrected by Bonferroni method. * represents a statistical difference compared with the R group, # represents a statistical difference compared between the M group and L group

Table 6: Comparison of the SUVmax values in the anterior, middle, and posterior parts of lumbar vertebrae.

Lumbar	Anterior	Middle	Posterior
L1 (n=36)	0.9 (0.73, 1.3)	1 (0.8, 1.28)*	0.9 (0.8, 1.2)
L2 (n=38)	1 (0.7, 1.2)	1 (0.8, 1.23)*	1 (0.8, 1.2) *
L3 (n=39)	1.1 (0.8, 1.3)	1.1 (0.9, 1.35)*	1 (0.9, 1.3) #
L4 (n=39)	1.2 (0.95, 1.4)	1.2 (1, 1.5)*	1.1 (1, 1.4) #
L5 (n=39)	1 (0.9, 1.4)	1.1 (0.9, 1.4)*	1 (0.9, 1.3) #

Note: Continuous variables were expressed as median values (Q1, Q3), and the pair comparison was corrected by the Bonferroni method. * represents a statistical difference compared with the Anterior group, # represents a statistical difference compared between the Middle group and the Posterior group

Table 7: Comparison of the SUVmean values in the anterior, middle, and posterior portions of lumbar vertebrae.

Lumbar	Anterior	Middle	Posterior
L1 (n=36)	0.7 (0.5, 0.88)	0.8 (0.6, 1)*	0.7 (0.6, 0.88)#
L2 (n=38)	0.7 (0.6, 1)	0.8 (0.6, 1)*	0.7 (0.6, 0.9)#
L3 (n=39)	0.8 (0.6, 1)	0.9 (0.7, 1.1)*	0.8 (0.6, 1)#
L4 (n=39)	0.9 (0.7, 1)	0.9 (0.8, 1.1)	0.8 (0.7, 1)
L5 (n=39)	0.8 (0.6, 1)	0.8 (0.7, 1.1)*	0.7 (0.6, 0.9)#

Note: Continuous variables were expressed as median (Q1, Q3), and the pair comparison was corrected by the Bonferroni method. * represents a statistical difference compared with the Anterior group, # represents a statistical difference compared between the Middle group and the Posterior group

Discussion

The SUV might be useful as an appropriate quantitative measure in skeletal SPECT/CT imaging and has been frequently used in evaluating the activities of bone lesions

Citation: Wang R, Shen C, Han D, Zhang Z, Feng Y, et al. (2021) A retrospective study of SPECT/CT scans using SUV measurement of the normal lumbar vertebrae with Tc-99m methylene diphosphonate. Int J Radiol Radiat Oncol 7(1): 022-029. DOI: https://dx.doi.org/10.17352/ijrro.000046

and the response to therapy [7,15,16]. Since the SUV reflects the osteoblastic activity, and the concentration of the bone-seeking agents would be directly correlated to the SUV [13,17]. However, It is difficult to determine a standard value for a normal bone since the measure was based on the body weight of the normal vertebrae with wide variability [5,18]. In this study, the SUVmax and SUVmean that were based on the body weight of various parts of the vertebral body such as anterior, middle, and posterior parts, and left, middle, and right segments of lumbar vertebra were calculated.

In this current study, there were no statistical differences in most SUVs of the upper, middle, and lower parts of the lumbar vertebral body. In the human vertebrae, the trabeculae's thickness and length of a normal cancellous bone designate the physiologic compressive and tension stresses of the bone. The trabeculae of a cancellous bone can remodel in orientation, number, and structure to accommodate and distribute the stresses to which the bone is exposed [19]. Therefore, the SUVs of the upper, middle and lower parts of the vertebral body might have shown no statistical difference. However, the SUVmax and SUVmean of the parts of the L1 and L2 vertebral body differed significantly from those of the other portions. Since the osteoporotic fractures occur most frequently in the thoracolumbar junction (T12 to L2) due to compression, the changes in both stresses and strains were most pronounced in the posterior part of the vertebral body in this specific area [20]. Banse, *et al.* [16] demonstrated that the vertical inhomogeneity was clearly pronounced in the images because the lower half of the vertebral body had a lower density than the upper half of the vertebral body. The differences ranged from 15% to 25% in their study. In the thoracolumbar and lumbar vertebrae, the numbers of nodes or node-to-node struts were two-fold higher in the inferior half than in the superior half of the vertebral body. The trabecular thickness and number of free-ends manifested a center or a close-to-endplate structural pattern, with the central trabeculae being 15% thicker than the close-to-endplate. Further, the central trabeculae had 30% fewer free-ends than the close-to-end plate in the same study [21]. These inferences might be the rationale for the difference in the SUVs between the upper and lower posterior segments of the L1 and L2 lumbar vertebrae. Additionally, the SUVmax of the middle portion of the L3 vertebral body had significant differences compared with the lower part and the upper part of the vertebral body. The L3 vertebral body differed in vertical inhomogeneity to a varying degree. The middle vertebral segment had more sparsely arranged trabeculae, higher porosity, and lower bone mass than the upper and lower segments of the vertebral body [22]. These characteristics of the cancellous bone of the middle segment explicate its minor role in load-bearing function. Similarly, the greatest proportion of load-bearing cortical bone appears in the smallest vertebral cross-section of the middle segment [23]. Mundinger *et al.* revealed that the trabeculae's microarchitectural pattern was fine near the endplates but coarse at the center of the vertebrae [24]. Our results were consistent with the results of these previous studies relevant to the biomechanical function stating that the *in vivo* loads are distributed differently at the endplates compared with the middle segment of the vertebra.

This current research showed that Significant differences were widely observed among SUVmax and SUVmean measures in the right, middle and left parts of the lumbar vertebrae (Table 4). The lumbar vertebral bodies have two ossification centers, which merge and form single ossification centers on each side of the vertebral arch [25]. The Tc-99m-DPD bone uptake depended on the bone osteoblastic activity, vascularization, and environmental factors [14]. In the present study, when the left, middle and right areas of interest of the vertebral body were sketched, the vertebral body was divided into three equal parts. The ossification centers of the left and the right vertebral bodies were included in the left and right areas of interest. Therefore, the SUVs on the left and right sides of the vertebral body were greater than the SUVs on the middle part of the vertebral body. The central belt of the vertebral body is where the ossifying centers of the two sides merge. This anatomical disposition may be the reason for the significant differences among the SUVmax in the right, middle and left portions of the lumbar vertebrae. With the advances in densitometric technologies and *ex vivo* analyses of the properties of a trabecular bone, it now becomes evident that the heterogeneity exists within the trabecular bone of a vertebral body [26]. The basis for the differences of the SUVmean in the right and left portions of the lumbar vertebrae may warrant further study.

The SUVmean and SUVmax measures in the middle of the vertebral body were significantly higher than those in the anterior and posterior parts of the lumbar vertebrae. There were significant differences among the SUVmean and SUVmax in the anterior, middle, and posterior portions of the lumbar vertebrae (Table 5). Banse *et al.* found that the structural differences between anterior, posterior, and external areas were inapparent and followed the density patterns. The cancellous bone density was 20% higher in the posterior cores than the anterior and external cores [21]. The regional morphometry and subregional density of the cancellous bones had significant differences with age and sex [26-28]. In the human vertebrae, the lumbar vertebrae play roles in both weight-bearing and load-transfer. The vertical bone trabeculae follow the lines of compressive stresses and are the primary load-bearing structure of the cancellous bone in the vertebrae, whereas the horizontal bone trabeculae are the main structure to distribute the stress and absorb the energy [19]. During aging, there is a non-uniform loss of bone within the vertebral body, resulting in non-homogeneous density throughout the centrum of the trabecular bone [19,29,30]. These sequels may have resulted from the regional compressive load-bearing and strong energy absorption capacity of the osteoporotic population.

The main limitation of the study subjects was tumor patients without bone metastasis, which might have an inapparent selective deviation from a typically normal bone. Further, this current study had a small sample size and the changes in the SUVs due to age and sex were not considered. The study also did not compare the trend in changes in the vertebral body among radio-chemotherapy patients. The diagnostic accuracy of the absence of metastasis warrants further verification in the present study.

Citation: Wang R, Shen C, Han D, Zhang Z, Feng Y, et al. (2021) A retrospective study of SPECT/CT scans using SUV measurement of the normal lumbar vertebrae with Tc-99m methylene diphosphonate. Int J Radiol Radiat Oncol 7(1): 022-029. DOI: https://dx.doi.org/10.17352/ijrro.000046

Conclusion

The difference in the bone metabolism of the lumbar vertebral body is caused by the variation in the horizontal direction of the vertebral body. The bone metabolism in the vertical direction of the lumbar vertebrae has more uniformity. As a quantitative imaging measure, the SUVs might require standardization with adequate reference data to minimize the variability in the participants.

Acknowledgments

This study was supported by funding from the Key research and development project of Shaanxi Province (2018SF-203). This study was supported by funding from the Shaanxi University of Chinese Medicine (No. 2016TY10). This study was supported by funding from the affiliated Hospital of Shaanxi University of Chinese Medicine (No. 2020MS020). This study was supported by funding from innovation team of Shaanxi University of Chinese Medicine(2019).

References

1. Macedo F, Ladeira K, Pinho F, Saraiva N, Bonito N, et al. (2017) Bone Metastases: An Overview. Oncol Rev 11: 321. Link: https://bit.ly/3ukhlpU

2. Rohani MFM, Yonan SNM, Tagiling N, Zainon Wmnw, Udin Y, et al. (2020) Standardized Uptake Value from Semiquantitative Bone Single-Photon Emission Computed Tomography/Computed Tomography in Normal Thoracic and Lumbar Vertebrae of Breast Cancer Patients. Asian Spine J 14: 629-638. Link: https://bit.ly/3rU9Og2

3. Bienz M, Saad F (2015) Management of bone metastases in prostate cancer: a review. Curr Opin Support Palliat Care 9: 261-267. Link: https://bit.ly/39JO8wK

4. Spinelli MS, Ziranu A, Piccioli A, Maccauro G (2016) Surgical treatment of acetabular metastasis. Eur Rev Med Pharmacol Sci 20: 3005-3010. Link: https://bit.ly/3wwkXqY

5. Kaneta T, Ogawa M, Daisaki H, Nawata S, Yoshida K, et al. (2016) SUV measurement of normal vertebrae using SPECT/CT with Tc-99m methylene diphosphonate. Am J Nucl Med Mol Imaging 6: 262-268. Link: https://bit.ly/3fLwBrO

6. Love C, Din AS, Tomas MB, Kalapparambath TP, Palestro CJ (2003) Radionuclide bone imaging: an illustrative review. Radiographics 23: 341-358. Link: https://bit.ly/3dBriZw

7. Wang R, Duan X, Shen C, Han D, Ma J, et al. (2018) A retrospective study of SPECT/CT scans using SUV measurement of the normal pelvis with Tc-99m methylene diphosphonate. J Xray Sci Technol 26: 895-908. Link: https://bit.ly/3wvbU9B

8. Sullivan DC, Obuchowski NA, Kessler LG, Raunig DL, Gatsonis C, et al. (2015) Metrology Standards for Quantitative Imaging Biomarkers. Radiology 277: 813-825. Link: https://bit.ly/3mneQ3q

9. Frank R, Group Fdg-Pet Ct Working (2008) Quantitative Imaging Biomarkers Alliance FDG-PET/CT Working Group report. Mol Imaging Biol 10: 305. Link: https://bit.ly/31NaRUb

10. Gerety EL, Lawrence EM, Wason J, Yan H, Hilborne S, et al. (2015) Prospective study evaluating the relative sensitivity of 18F-NaF PET/CT for detecting skeletal metastases from renal cell carcinoma in comparison to multidetector CT and 99mTc-MDP bone scintigraphy, using an adaptive trial design. Ann Oncol 26: 2113-2118. Link: https://bit.ly/3dFCnZh

11. Huang K, Feng Y, Liu D, Liang W, Li L (2020) Quantification evaluation of (99m) Tc-MDP concentration in the lumbar spine with SPECT/CT: compare with bone mineral density. Ann Nucl Med 34: 136-143. Link: https://bit.ly/3rUvDvG

12. Qi N, Meng Q, You Z, Chen H, Shou Y, et al. (2021) Standardized uptake values of (99m)Tc-MDP in normal vertebrae assessed using quantitative SPECT/CT for differentiation diagnosis of benign and malignant bone lesions. BMC Med Imaging 21: 39. Link: https://bit.ly/3cUzQeK

13. Hirschmann MT, Davda K, Rasch H, Arnold MP, Friederich NF (2011) Clinical value of combined single photon emission computerized tomography and conventional computer tomography (SPECT/CT) in sports medicine. Sports Med Arthrosc Re 19: 174-181. Link: https://bit.ly/3dEpiiV

14. Tabotta F, Jreige M, Schaefer N, Becce F, Prior JO, et al. (2019) Quantitative bone SPECT/CT: high specificity for identification of prostate cancer bone metastases. BMC Musculoskelet Disord 20: 619. Link: https://bit.ly/3upQKYz

15. Doddala SM, Suryadevara A, Chinta SK, Madisetty AL (2016) Incidence and pattern of bone metastases at presentation in Indian carcinoma breast patients. Indian J Cancer 53: 360-362. Link: https://bit.ly/2PuXdTt

16. Kuji I, Yamane T, Seto A, Yasumizu Y, Shirotake S, et al. (2017) Skeletal standardized uptake values obtained by quantitative SPECT/CT as an osteoblastic biomarker for the discrimination of active bone metastasis in prostate cancer. Eur J Hybrid Imaging 1: 2. Link: https://bit.ly/3mmCSvr

17. Mohd Rohani MF, Mat Nawi N, Shamim SE, Wan Sohaimi WF, Wan Zainon WMN, et al. (2020) Maximum standardized uptake value from quantitative bone single-photon emission computed tomography/computed tomography in differentiating metastatic and degenerative joint disease of the spine in prostate cancer patients. Ann Nucl Med 34: 39-48. Link: https://bit.ly/3fRcLvz

18. Adams MC, Turkington TG, Wilson JM, Wong TZ (2010) A systematic review of the factors affecting accuracy of SUV measurements. AJR Am J Roentgenol 195: 310-320. Link: https://bit.ly/2R6DxFH

19. Wang Y, Liu G, Li T, Xiao Y, Han Q, et al. (2010) Morphometric comparison of the lumbar cancellous bone of sheep, deer, and humans. Comp Med 60: 374-379. Link: https://bit.ly/3rU1vRd

20. Erdem I, Truumees E, van der Meulen MC (2013) Simulation of the behaviour of the L1 vertebra for different material properties and loading conditions. Comput Methods Biomech Biomed Engin 16: 736-746. Link: https://bit.ly/2Onhx8u

21. Banse X, Devogelaer JP, Munting E, Delloye C, Cornu O, et al. (2001) Inhomogeneity of human vertebral cancellous bone: systematic density and structure patterns inside the vertebral body. Bone 28: 563-571. Link: https://bit.ly/3mvySZK

22. Gibson LJ (1985) The mechanical behaviour of cancellous bone. J Biomech 18: 317-328. Link: https://bit.ly/31SNfhb

23. Eswaran SK, Gupta A, Adams MF, Keaveny TM (2006) Cortical and trabecular load sharing in the human vertebral body. J Bone Miner Res 21: 307-314. Link: https://bit.ly/3cPhLi9

24. Mundinger A, Wiesmeier B, Dinkel E, Helwig A, Beck A, et al. (1993) Quantitative image analysis of vertebral body architecture--improved diagnosis in osteoporosis based on high-resolution computed tomography. Br J Radiol 66: 209-213. Link: https://bit.ly/3cR2WM8

25. Chaturvedi A, Klionsky NB, Nadarajah U, Chaturvedi A, Meyers SP (2018) Malformed vertebrae: a clinical and imaging review. Insights Imaging 9: 343-355. Link: https://bit.ly/3rRd0J5

26. Briggs AM, Greig AM, Wark JD, Fazzalari NL, Bennell KL (2004) A review of anatomical and mechanical factors affecting vertebral body integrity. Int J Med Sci 1: 170-180. Link: https://bit.ly/2R2qUvi

27. Duan Y, Parfitt AM, Seeman E (1999) Vertebral bone mass, size, and volumetric density in women with spinal fractures. J Bone Miner Res 14: 1796-1802. Link: https://bit.ly/3fHCkyZ

Citation: Wang R, Shen C, Han D, Zhang Z, Feng Y, et al. (2021) A retrospective study of SPECT/CT scans using SUV measurement of the normal lumbar vertebrae with Tc-99m methylene diphosphonate. Int J Radiol Radiat Oncol 7(1): 022-029. DOI: https://dx.doi.org/10.17352/ijrro.000046

28. Gong H, Zhang M, Yeung HY, Qin L (2005) Regional variations in microstructural properties of vertebral trabeculae with aging. J Bone Miner Metab 23: 174-180. Link: https://bit.ly/3sTyrdT

29. Antonacci MD, Hanson DS, Leblanc A, Heggeness MH (1997) Regional variation in vertebral bone density and trabecular architecture are influenced by osteoarthritic change and osteoporosis. Spine (Phila Pa 1976) 22: 2393-2401. Link: https://bit.ly/3dF9PPI

30. McCubbrey DA, Cody DD, Peterson EL, Kuhn JL, Flynn MJ, et al. (1995) Static and fatigue failure properties of thoracic and lumbar vertebral bodies and their relation to regional density. J Biomech 28: 891-899. Link: https://bit.ly/3wyultS

Citation: Wang R, Shen C, Han D, Zhang Z, Feng Y, et al. (2021) A retrospective study of SPECT/CT scans using SUV measurement of the normal lumbar vertebrae with Tc-99m methylene diphosphonate. Int J Radiol Radiat Oncol 7(1): 022-029. DOI: https://dx.doi.org/10.17352/ijrro.000046